The Astrophysical Journal Letters, 881:L1 (5pp), 2019 August 10 https://doi.org/10.3847/2041-8213/ab339b

Most Black Holes Are Born Very Slowly Rotating

Jim Fuller[1] and Linhao Ma[1,2]
[1] TAPIR, Mailcode 350-17, California Institute of Technology, Pasadena, CA 91125, USA; jfuller@caltech.edu
[2] Department of Modern Physics, University of Science and Technology of China, Hefei, Anhui 230026, People's Republic of China
Received 2019 June 4; revised 2019 July 17; accepted 2019 July 18; published 2019 August 5

Abstract

The age of gravitational-wave astronomy has begun, and black hole (BH) mergers detected by the Laser Interferometer Gravitational-Wave Observatory (LIGO) are providing novel constraints on massive star evolution. A major uncertainty in stellar theory is the angular momentum (AM) transport within the star that determines its core rotation rate and the resulting BH's spin. Internal rotation rates of low-mass stars measured from asteroseismology prove that AM transport is efficient, suggesting that massive stellar cores may rotate slower than prior expectations. We investigate AM transport via the magnetic Tayler instability, which can largely explain the rotation rates of low-mass stars and white dwarfs. Implementing an updated AM transport prescription into models of high-mass stars, we compute the spins of their BH remnants. We predict that BHs born from single stars rotate very slowly, with $a \sim 10^{-2}$, regardless of initial rotation rate, possibly explaining the low $\chi_{\rm eff}$ of most BH binaries detected by LIGO thus far. A limited set of binary models suggests slow rotation for many binary scenarios as well, although homogeneous evolution and tidal spin-up of post-common-envelope helium stars can create moderate or high BH spins. We make predictions for the values of $\chi_{\rm eff}$ in future LIGO events, and we discuss implications for engine-powered transients.

Unified Astronomy Thesaurus concepts: Massive stars (732); Stellar mass black holes (1611); Stellar rotation (1629); Rotating black holes (1406); Stellar evolutionary models (2046); Solar evolution (1492); Magnetohydrodynamics (1964); Astrophysical fluid dynamics (101)

1. Introduction

Spin is one of only three fundamental properties of black holes (BHs), but there are few reliable predictions of natal BH spins. The BH spin is determined by the angular momentum (AM) content of the core of the star that collapses into the BH. Yet our ability to predict internal stellar rotation rates and AM content has been limited by sparse observational constraints and the complex magnetohydrodynamics of differentially rotating stars. Without any AM transport within the star, nearly all compact objects would be born maximally rotating (Heger et al. 2000), but efficient AM transport will couple the stellar core and envelope, slowing the spin of the core and its compact object descendant.

Measurements of nonaccreting stellar-mass BH spins are now possible for merging BHs detected by the Laser Interferometer Gravitational-Wave Observatory (LIGO; Abbott et al. 2016; The LIGO Scientific Collaboration et al. 2018a). Most of these BHs are consistent with very low spin (Roulet & Zaldarriaga 2019; The LIGO Scientific Collaboration et al. 2018b), though there appear to be a small fraction of moderately or rapidly rotating systems (e.g., Zackay et al. 2019). BH spins can also be measured in X-ray binaries (XRBs), and current estimates suggest a broad range of spin rates ($0.1 \lesssim a \lesssim 1$; Miller & Miller 2015). However, XRB BH spin rates are complicated by difficult accretion disk modeling that sometimes yields conflicting results, and spins can be increased by prior/ongoing accretion (Fragos & McClintock 2015).

Until recently, it was extremely challenging to observationally constrain AM transport within stars. Fortunately, asteroseismology has delivered decisive data (Beck et al. 2012; Mosser et al. 2012; Deheuvels et al. 2015; Hermes et al. 2017; Gehan et al. 2018), unambiguously demonstrating that the internal rotation rates of low-mass stars (and their white dwarf descendants) are slower than predicted by essentially all previous models (e.g., Heger et al. 2005; Meynet & Maeder 2005; Woosley & Heger 2006; Cantiello et al. 2014; Wheeler et al. 2015). Most prior predictions of internal stellar rotation rates and natal neutron star (NS)–BH spins are therefore unreliable and could be overestimated. Models based on the Tayler–Spruit dynamo (Spruit 2002), such as Heger et al. (2005) and Qin et al. (2018), predicted fairly slow rotation ($a \lesssim 0.1$) for BHs born from single stars; thus, many BHs are likely to rotate even slower than those estimates.

In low-mass stars, AM is transported from the rapidly rotating core to the slowly rotating envelope, decreasing the spin of the stellar core and its white dwarf descendant. In a recent paper, Fuller et al. (2019) demonstrated that internal rotation rates of low-mass stars can potentially be explained by magnetic torques arising from the Tayler instability (e.g., Spruit 1999), but with a different nonlinear saturation mechanism than that proposed by Spruit (2002), increasing AM transport and decreasing core rotation rates. Here, we extend the calculations of Fuller et al. (2019) to high-mass stars to predict the AM contained in the core of the star, and hence the spin of the BH that is formed upon its collapse.

2. Computations

2.1. AM Transport

Our stellar models include internal AM transport according to the same prescription as Fuller et al. (2019) based on magnetic torques arising from the Tayler instability. These torques are larger than those predicted by the Tayler–Spruit dynamo of Spruit (2002) due to a larger saturation amplitude of the Tayler instability arising from weaker nonlinear damping, as elaborated in Fuller et al. (2019). In radiative zones, AM is

Table 1
Spin Results for Stellar Models Described in the Text

$M_i/M_\odot$	$Z/Z_\odot$	$M_{\rm He}/M_\odot$	$a_{\rm He}$	Evolution
12	1.2	3.5	0.006	Single
14	1.2	4.2	0.007	Single
16	1.2	4.9	0.007	Single
18	1.2	5.8	0.008	Single
20	1.2	6.7	0.009	Single
25	1.2	9.0	0.009	Single
30	1.2	10.7	0.010	Single
40	0.5	16.5	0.003	Single
40	0.1	19.1	0.014	Single
40	0.01	21.4	0.010	Single
40	0.5	13.6	0.050	Case A
40	0.5	15.2	0.009	Case B (stable)
40	0.5	12.3	0.018	Case B (unstable)
40	0.5	12.1	0.513	Case B (tide)
40	0.012	31.4	0.549	Homogeneous
45	1.2	17.6	0.010	Single
60	0.5	26.6	0.006	Single
75	0.5	35.2	0. 35	Single

Note. The columns show the initial stellar mass, metallicity, final helium core mass, final helium core dimensionless spin, and the type of single/binary evolution.

transported by an effective viscosity

$$\nu_{\rm AM} = r^2\Omega\left(\frac{\Omega}{N_{\rm eff}}\right)^2, \quad (1)$$

where r is the radial coordinate, Ω is the local angular rotation frequency, $N_{\rm eff} \approx N_\mu$ is the effective Brunt–Väisälä frequency, and N_μ is the compositional part of the Brunt–Väisälä frequency. AM is only transported via Equation (1) if the local shear $q = d\ln\Omega/d\ln r$ is above the critical value

$$q_{\rm min} = \left(\frac{N_{\rm eff}}{\Omega}\right)^{5/2}\left(\frac{\eta}{r^2\Omega}\right)^{3/4}, \quad (2)$$

where η is the magnetic diffusivity. Stellar models with this prescription provide a reasonable match with data for low-mass stars. In convective zones, AM is transported via an effective convective viscosity that enforces nearly rigid rotation.

2.2. Stellar Models

We construct stellar models with the MESA stellar evolution code (Paxton et al. 2011, 2013, 2015, 2018), implementing the AM viscosity above. We study single stars with initial masses ranging from $12 \leqslant M_i \leqslant 75\,M_\odot$ and metallicities from $0.1Z_\odot \leqslant Z \leqslant 1.2Z_\odot$ and initial equatorial rotation speed $v_{\rm rot} = 150\,{\rm km\,s^{-1}}$. All models are listed in Table 1. Our models include moderate convective overshoot (with exponential overshooting parameter $f = 0.025$) and mass loss via the "Dutch" prescription (with efficiency $\eta = 0.5$). We run our models from the zero-age main sequence (ZAMS) to core carbon depletion, after which we do not expect significant changes in the helium core mass $M_{\rm He}$ or AM content $J_{\rm He}$.

In addition to the single-star models listed in Table 1, we have run several binary models involving a 40 $M_\odot$ primary. In each of these models, tidal spin-up and mass transfer are included via the prescriptions of Qin et al. (2018). In the "Case A" scenario, the primary begins in a 3 day orbit with a companion of 20 $M_\odot$, such that mass transfer (which is assumed to be fully conservative) begins on the main sequence. In the "Case B (stable)" scenario, the initial orbital period is instead 50 days such that Roche-lobe overflow occurs soon after the main sequence while the donor is radiative and the mass transfer is stable. In the "Case B (unstable)" scenario, the initial orbital period is 1000 days, Roche-lobe overflow occurs when the star has expanded into a red supergiant with a convective envelope, and the mass transfer is unstable. For this model, the hydrogen envelope is removed upon Roche-lobe overflow, and the binary period is set to 3 days. The "Case B (tide)" scenario is the same, except the post-common-envelope period is set to 0.5 days such that tides spin up the helium star. Finally, in the "Homogeneous" scenario, the companion mass is 40 $M_\odot$ and the initial orbital period is 1.5 days. Rotational mixing is included in this model (via MESA's default Eddington–Sweet mixing scheme) and causes the star to evolve quasi-homogeneously (Maeder 1987; Woosley & Heger 2006; Yoon et al. 2006; de Mink et al. 2009; Mandel & de Mink 2016).

3. Results

Some massive stars, especially stars with initial masses $M \gtrsim 20\,M_\odot$, produce BHs upon core collapse. The resulting stellar remnant is a rotating Kerr BH, whose dimensionless spin a is defined as

$$a \equiv \frac{Jc}{GM^2}, \quad (3)$$

where J is the AM of the BH. When core-collapse explosion fails and a BH is formed, the sudden loss of mass from radiated neutrinos generates a weak shock that can still unbind the hydrogen envelope of the star (Nadezhin 1980; Lovegrove & Woosley 2013). In red supergiants, the shock unbinds the majority of the hydrogen envelope, though blue supergiants will retain most of their hydrogen (Fernández et al. 2018). Most of our models are red supergiants or have very little remaining hydrogen at the time of collapse, so we assume that only mass within the helium core will fall into the BH. Hence, when computing BH masses and spins, we use the mass $M_{\rm He}$ and AM $J_{\rm He}$ in the helium core, which we define as the mass coordinate below which the hydrogen mass fraction falls below 10^{-2}.

Figure 1 shows the dimensionless spin and specific AM of the helium core of several 40 $M_\odot$ models. When it first forms at the end the main sequence, the helium core has enough AM to produce a maximally rotating BH with $a \simeq 1$. However, similar to the results of Fuller et al. (2019) for low-mass stars, the vast majority the helium core's AM is removed during hydrogen shell-burning as the helium core contracts and spins up. The internal shear activates the Tayler instability that counteracts the core spin-up, transporting AM from the helium core to the hydrogen envelope. The core's AM is further depleted by a factor of a few between helium exhaustion and core collapse.

The final BH spins of our single-star models is typically $a \lesssim 10^{-2}$, i.e., nearly nonrotating. Figure 2 shows our predictions for the dimensionless BH spin $a_{\rm He}$ for each of our models, assuming mass within the helium core collapses into a BH (though the models with $M_{\rm He} \lesssim 5\,M_\odot$ may be more likely to form NSs). We have run models with ZAMS rotational velocities of 50, 150, and 450 $\rm km\,s^{-1}$, but we find

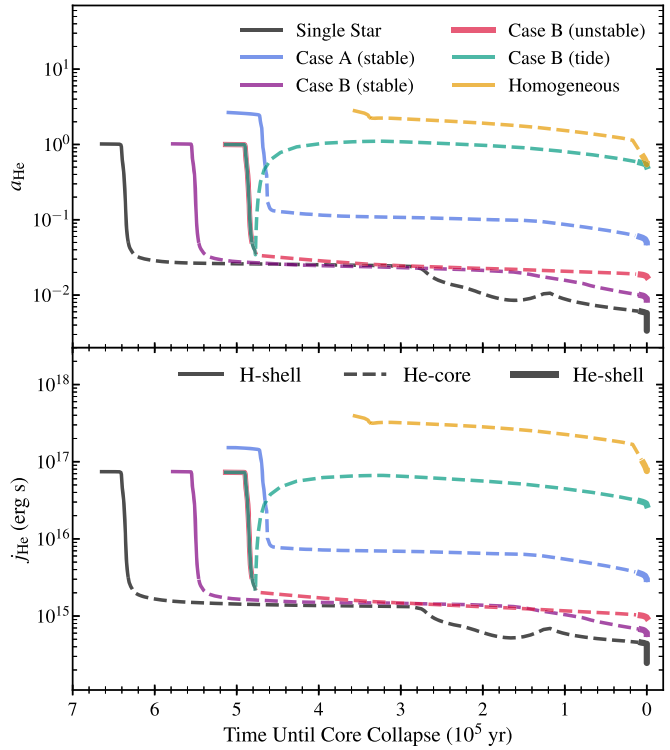

Figure 1. Top: dimensionless spin $a = J_{\rm He}c/(GM_{\rm He}^2)$ of the helium core of $40M_\odot$ progenitors as they evolve, from the end of the main sequence until carbon depletion. Each line corresponds to a single/binary scenario as discussed in the text. The line styles represent evolutionary phases corresponding to hydrogen shell-burning (solid lines), core helium-burning (dashed lines), and helium shell-burning (thick lines). If only the mass and AM of the helium core falls into the BH, the resulting spin is expected to be very small, except in a binary scenario where a helium star is tidally spun up (green line), or a homogeneous evolutionary scenario (yellow line). Bottom: the corresponding specific AM of the helium core, $j_{\rm He} = J_{\rm He}/M_{\rm He}$. The sudden "cliff" in specific AM occurs just after the main sequence, when the helium core contracts as the star crosses the Hertzsprung gap.

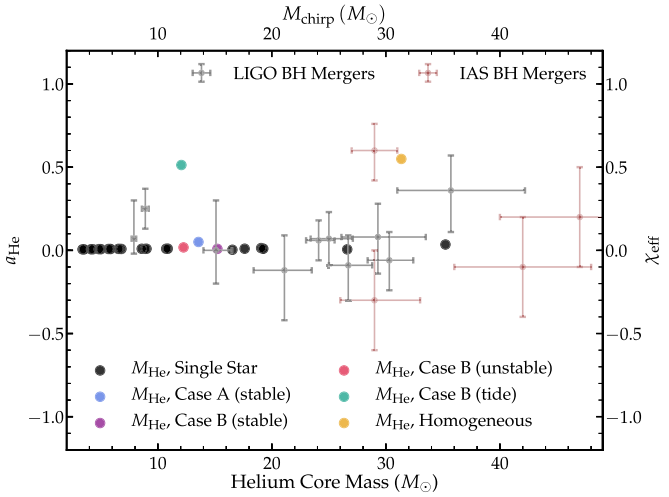

Figure 2. Dimensionless spin, $a_{\rm He}$, of the helium core just before core collapse as a function final helium core mass, with points corresponding to the models listed in Table 1. On the upper x-axis and right y-axis, we show the chirp masses and $\chi_{\rm eff}$ values for BH mergers detected by LIGO (Abbott et al. 2016; The LIGO Scientific Collaboration et al. 2018a; gray crosses) and additional mergers from the Institute for Advanced Study group (pale red crosses; Venumadhav et al. 2019; Zackay et al. 2019). For single stars (black points), if a black hole is formed upon core collapse, we generally predict $a \sim 10^{-2}$ if only material in the helium core falls into the black hole. The colored points correspond to the same binary models shown in Figure 1. Only binary models with post-common-envelope tidal spin-up or homogeneous evolution are capable of producing moderate or large spins.

the initial rotation rate has almost no effect on the final value of $a_{\rm He}$, similar to low-mass stellar models. Hence, we generally predict very slow natal spins of BHs stemming from single stars near solar metallicity. A few runs at much lower metallicity also produce very slowly rotating BHs, though with slightly larger spins due to less mass loss.

Certain types of binary evolution may produce much more rapidly rotating BHs. Figure 1 shows how the helium core AM evolves in various binary scenarios, with final spins shown as colored points in Figure 2. We predict slow BH rotation for many binaries evolving through Case A and Case B mass transfer. Even though the hydrogen envelope is eventually stripped from these models, it is still able to absorb most of the helium core's AM before it is removed, such that we still predict very slow BH rotation. There are two evolutionary scenarios that likely can result in rapid BH rotation. First, tidal spin-up of a helium star (our Case B tide model) in a short-period ($P \lesssim 1$ day), post-common-envelope binary can greatly increase its AM, and hence $a_{\rm He}$ (e.g., Kushnir et al. 2016). Second, very massive, low-metallicity, and short-period binaries that evolve quasi-homogeneously never develop a core-envelope structure. The entire star is burned to helium, so the core never loses AM to an extended hydrogen envelope, allowing it to remain rapidly rotating until core collapse to form a high-spin BH.

4. Discussion

The slow natal spins predicted by our models could explain the low values of the aligned spin component $\chi_{\rm eff}$ observed for most BH mergers detected by LIGO (The LIGO Scientific Collaboration et al. 2018a), shown in Figure 2. Indeed, several recent analyses (Farr et al. 2018; Roulet & Zaldarriaga 2019; The LIGO Scientific Collaboration et al. 2018b) have shown that the distribution of $\chi_{\rm eff}$ implies low spins ($a \lesssim 0.1$) if the spins of the BHs are aligned with their orbit, as expected for standard binary formation mechanisms in the field (Kalogera 2000) unless natal BH kicks are very large. Large BH spins are disfavored even for an isotropic distribution of spins as expected from BHs dynamically formed in dense stellar clusters (Roulet & Zaldarriaga 2019; The LIGO Scientific Collaboration et al. 2018b), and distributions with very low BH spins are tentatively most preferred, regardless of spin–orbit inclination (The LIGO Scientific Collaboration et al. 2018b). Our results, combined with the low $\chi_{\rm eff}$ of most LIGO events, suggest that most BHs are born with low spins and that low-spin priors should be considered when analyzing LIGO data.

It may be difficult to use spin alignment to disentangle BH mergers formed via field binaries from those formed via dynamical interactions (e.g., Rodriguez et al. 2016). If most BHs rotate very slowly, LIGO data cannot distinguish aligned and misaligned systems as expected from the field and cluster scenarios, respectively. A possible corollary of our results is that merging BHs with moderate or large $\chi_{\rm eff}$ formed from field binaries, because dynamically assembled BH binaries were not formed in tight binaries and should have very low spin. However, a caveat is the population of rapidly rotating ($a \sim 0.7$) BH primaries expected for second-generation cluster mergers (Antonini & Rasio 2016; Fishbach et al. 2017; Gerosa & Berti 2017; Rodriguez et al. 2018). Still, very high-spin mergers ($\chi_{\rm eff} \gtrsim 0.6$) are difficult to explain via second-

generation mergers and likely form via homogeneous evolution in which both BHs form with large spin. BH mergers with negative values of $\chi_{\rm eff}$ like GW170121 (Venumadhav et al. 2019) or with large misaligned spin $\chi_{\rm p}$ may form primarily via misaligned second-generation cluster mergers.

The LIGO data exhibit three events (the controversial GW151216 of Zackay et al. 2019, the Boxing Day event GW151226, and the high-mass event GW170729), which exhibit moderate spins inconsistent with zero at 90% confidence, though both GW151216 and GW170729 are lower significance events. Such moderate spin could be produced if one of the progenitor stars is spun up by tidal evolution and produces a rapidly rotating BH, while the other BH is slowly rotating. Indeed, our Case B (tide) point in Figure 2 is similar to the measured spin of GW151226 if only the secondary is rotating such that the measured $\chi_{\rm eff}$ is reduced by a factor $M_2/(M_1+M_2)$. A naive prediction of this tidal spin-up is that $\chi_{\rm eff}$ should exhibit a bimodal distribution with peaks at very slow spins due to binaries wide enough to avoid tidal synchronization, and moderate spins due to binaries where the second star was tidally synchronized (Zaldarriaga et al. 2018). While Qin et al. (2018) and Bavera et al. (2019) predict a more continuous distribution, future detections will help distinguish different evolutionary pathways (Stevenson et al. 2017; Talbot & Thrane 2017; Farr et al. 2018; Gerosa et al. 2018).

In these compact binaries, a weak explosion that generates a large amount of fallback material could moderately increase the BH spin above our estimates, because the fallback material is tidally torqued by the companion (Batta et al. 2017; Schrøder et al. 2018). Alternatively, loss of mass/AM from material with enough AM to form an accretion disk around the BH could moderately decrease the BH spin (Batta & Ramirez-Ruiz 2019). Similar to prior works, we predict a population of moderately rotating ($\chi_{\rm eff}\sim 0.1$–0.5) BHs at a wide range of masses formed via the tidal spin-up scenario. Bavera et al. (2019) predict that roughly 40% of BH mergers detected by advanced LIGO should have $\chi_{\rm eff}>0.1$ due to this evolutionary channel.

Forming binaries with very large spin $\chi_{\rm eff}\sim 1$ requires two aligned and rapidly rotating BHs if the mass ratio is near unity. The only model of which we are aware that can produce such events in the face of efficient AM transport is the chemically homogeneous scenario (e.g., de Mink & Mandel 2016; Mandel & de Mink 2016; Marchant et al. 2017). Hence, observations of $\chi_{\rm eff}\sim 1$ events may provide strong support for the homogeneous evolution scenario. The BH merger candidate GW151216 (Zackay et al. 2019) and GW170729 are the best candidates for homogeneous evolution thus far, and both events lie close to our Homogeneous point in Figure 2. Because the homogeneous evolution channel can only produce somewhat massive BHs, we predict an absence of highly spinning $\chi_{\rm eff}\sim 1$ and low-mass ($M_{\rm chirp}\lesssim 25\,M_\odot$) events. Homogeneous evolution can produce either slow or moderate rotation when stellar metallicity is not small and stellar winds carry away most of the stars' AM during core helium-burning. Hence, at high masses ($M_{\rm chirp}\gtrsim 30\,M_\odot$), it may be difficult to distinguish the tidal and homogeneous scenarios for moderately rotating BHs, but very large spins would be strong evidence for homogeneous evolution. While our homogeneous model resulted in a BH with $a\approx 0.5$, a model with less mass loss could yield $a>1$, and it is possible that homogeneous evolution will produce a pileup of systems with $\chi_{\rm eff}\approx 1$.

Our results are in tension with the apparent high spins inferred for BHs in XRBs (see Miller & Miller 2015 for a review). We are slightly skeptical of those model-dependent and sometimes contradictory measurements, which unfortunately cannot be calibrated against model-independent spin measurements. While the spins of BHs in low-mass XRBs could be increased by accretion of AM after formation (Fragos & McClintock 2015; though see also King & Kolb 1999), the spins of BHs in high-mass XRBs must be natal. It is difficult to reconcile measurements of high-spin BHs in high-mass XRBs with efficient AM transport (Qin et al. 2019), or with the slow spins of neutron stars (Miller et al. 2011). One possibility is that a significant amount of hydrogen falls back onto BHs upon formation, increasing their spins above our estimates. However, measurements only exist for binary systems where most of the hydrogen envelope was likely stripped before core collapse, potentially undermining the fallback spin-up mechanism.

Rotating blue supergiants, such as the progenitor of SN 1987A, may also give rise to rapidly rotating BHs. For these stars, neutrino-mediated mass loss will fail to unbind most of the hydrogen envelope (Fernández et al. 2018), and a rapidly rotating BH will be produced if the AM in the hydrogen envelope is accreted by the BH. However, because collapsing blue supergiants likely formed as a result of a prior binary interaction (Podsiadlowski 1992), few binary scenarios predict them to be the progenitors of BH mergers or XRBs, though they could plausibly be progenitors of ultra-long gamma-ray bursts. However, engine-driven transients such as long gamma-ray bursts, broad-lined SNe Ic, and superluminous SNe Ic do not show evidence for any hydrogen in their progenitor stars. These transients are likely driven by a rapidly rotating central engine from a (mostly) carbon–oxygen progenitor star (see the recent review in Fryer et al. 2019). Our results suggest these events are unlikely to originate from single stars, except at very low metallicity ($Z\lesssim 0.004$) where homogeneous evolution can occur for single stars (Yoon et al. 2006). Hence, we expect most engine-driven transients are likely produced via tidally spun-up Wolf–Rayet stars or stars evolving through homogeneous evolution.

Finally, the only competing AM transport model that may be able to explain the internal rotation rates of low-mass evolved stars is that of Kissin & Thompson (2015), in which stellar radiative zones rotate nearly rigidly and significant differential rotation exists in the convection zone. This model often predicts slow compact object rotation rates (Kissin & Thompson 2018), but predicts rapid core rotation in some cases. To compare with our predictions here, future work should investigate BH rotation rates for that scenario in more detail.

5. Conclusion

Asteroseismic data for low-mass stars (e.g., Deheuvels et al. 2015; Hermes et al. 2017; Gehan et al. 2018) have convincingly demonstrated that the cores of low-mass stars rotate at least an order of magnitude slower than predicted by most prior stellar models (Cantiello et al. 2014). Previous works on massive stars (e.g., Heger et al. 2005; Hirschi et al. 2005; Woosley & Heger 2006) are based on physics that overpredict core rotation rates for low-mass stars; hence, their predictions of compact object rotation rates are unreliable. We have reexamined BH natal spins using AM transport via magnetic torques arising from the Tayler instability (Spruit 1999, 2002),

based on an updated prescription that largely matches asteroseismic data for low-mass stars and white dwarfs (Fuller et al. 2019). In massive stars, we find magnetic torques extract most of the AM from the helium core just after the main sequence.

We predict extremely slow rotation $a \sim 10^{-2}$ for BHs born from single stars. We believe such AM transport is likely to be responsible for the low $\chi_{\rm eff}$ of most merging BHs detected by LIGO thus far (Roulet & Zaldarriaga 2019; The LIGO Scientific Collaboration et al. 2018b), regardless of a field binary or dynamical origin. Our preliminary investigation of BHs resulting from various binary pathways shows that very low spins are often produced in these scenarios as well. Hence, we predict that most of the LIGO BH population will be consistent with zero spin even with significantly smaller uncertainties in $\chi_{\rm eff}$. Two evolutionary scenarios leading to moderate/high BH spin are tidal torques that spin up a helium star in a short-period orbit after a common-envelope event (Kushnir et al. 2016; Qin et al. 2018), or rapid rotation (likely enforced by tidal spin-up) and low metallicity that allows for homogeneous evolution (Maeder 1987; Woosley & Heger 2006; Yoon et al. 2006). Both scenarios can produce moderate ($a \sim 0.1$–0.5) BH spins, but only homogeneous evolution can produce very large spins with $a \sim 1$, though it should only occur for high-chirp-mass ($M_{\rm chirp} \gtrsim 25\,M_{\odot}$) mergers.

A corollary to our results is that BH mergers with moderate or large values of $\chi_{\rm eff}$ likely originated from tidally spun-up field binaries or second-generation cluster mergers. A second corollary is that gamma-ray bursts and other high-energy transients powered by rapidly rotating compact objects are likely to be formed in binaries from one of the two tidal spin-up scenarios discussed above. Future work should investigate fallback effects, examine stars with very low metallicities, and make predictions for a general population of binaries.

We thank Will Farr, Davide Gerosa, Greg Salvesen, and Christopher Berry for enlightening conversations. This research is funded in part by an Innovator Grant from The Rose Hills Foundation and the Sloan Foundation through grant FG-2018-10515.

ORCID iDs

Jim Fuller https://orcid.org/0000-0002-4544-0750

References

Abbott, B. P., Abbott, R., Abbott, T. D., et al. 2016, PhRvX, 6, 041015
Antonini, F., & Rasio, F. A. 2016, ApJ, 831, 187
Batta, A., & Ramirez-Ruiz, E. 2019, arXiv:1904.04835
Batta, A., Ramirez-Ruiz, E., & Fryer, C. 2017, ApJL, 846, L15
Bavera, S. S., Fragos, T., Qin, Y., et al. 2019, arXiv:1906.12257
Beck, P. G., Montalban, J., Kallinger, T., et al. 2012, Natur, 481, 55
Cantiello, M., Mankovich, C., Bildsten, L., et al. 2014, ApJ, 788, 93
Deheuvels, S., Ballot, J., Beck, P. G., et al. 2015, A&A, 580, A96
de Mink, S. E., Cantiello, M., Langer, N., et al. 2009, A&A, 497, 243
de Mink, S. E., & Mandel, I. 2016, MNRAS, 460, 3545
Farr, B., Holz, D. E., & Farr, W. M. 2018, ApJL, 854, L9
Fernández, R., Quataert, E., Kashiyama, K., & Coughlin, E. R. 2018, MNRAS, 476, 2366
Fishbach, M., Holz, D. E., & Farr, B. 2017, ApJL, 840, L24
Fragos, T., & McClintock, J. E. 2015, ApJ, 800, 17
Fryer, C. L., Lloyd-Ronning, N., Wollaeger, R., et al. 2019, arXiv:1904.10008
Fuller, J., Piro, A. L., & Jermyn, A. S. 2019, MNRAS, 485, 3661
Gehan, C., Mosser, B., Michel, E., et al. 2018, A&A, 616, A24
Gerosa, D., & Berti, E. 2017, PhRvD, 95, 124046
Gerosa, D., Berti, E., O'Shaughnessy, R., et al. 2018, PhRvD, 98, 084036
Heger, A., Langer, N., & Woosley, S. E. 2000, ApJ, 528, 368
Heger, A., Woosley, S. E., & Spruit, H. C. 2005, ApJ, 626, 350
Hermes, J. J., Gänsicke, B. T., Kawaler, S. D., et al. 2017, ApJS, 232, 23
Hirschi, R., Meynet, G., & Maeder, A. 2005, A&A, 443, 581
Kalogera, V. 2000, ApJ, 541, 319
King, A. R., & Kolb, U. 1999, MNRAS, 305, 654
Kissin, Y., & Thompson, C. 2015, ApJ, 808, 35
Kissin, Y., & Thompson, C. 2018, ApJ, 862, 111
Kushnir, D., Zaldarriaga, M., Kollmeier, J. A., & Waldman, R. 2016, MNRAS, 462, 844
Lovegrove, E., & Woosley, S. E. 2013, ApJ, 769, 109
Maeder, A. 1987, A&A, 178, 159
Mandel, I., & de Mink, S. E. 2016, MNRAS, 458, 2634
Marchant, P., Langer, N., Podsiadlowski, P., et al. 2017, A&A, 604, A55
Meynet, G., & Maeder, A. 2005, A&A, 429, 581
Miller, J. M., Miller, M. C., & Reynolds, C. S. 2011, ApJL, 731, L5
Miller, M. C., & Miller, J. M. 2015, PhR, 548, 1
Mosser, B., Goupil, M. J., Belkacem, K., et al. 2012, A&A, 548, A10
Nadezhin, D. K. 1980, Ap&SS, 69, 115
Paxton, B., Bildsten, L., Dotter, A., et al. 2011, ApJS, 192, 3
Paxton, B., Cantiello, M., Arras, P., et al. 2013, ApJS, 208, 4
Paxton, B., Marchant, P., Schwab, J., et al. 2015, ApJS, 220, 15
Paxton, B., Schwab, J., Bauer, E. B., et al. 2018, ApJS, 234, 34
Podsiadlowski, P. 1992, PASP, 104, 717
Qin, Y., Fragos, T., Meynet, G., et al. 2018, A&A, 616, A28
Qin, Y., Marchant, P., Fragos, T., et al. 2019, ApJL, 870, L18
Rodriguez, C. L., Amaro-Seoane, P., Chatterjee, S., et al. 2018, PhRvL, 120, 151101
Rodriguez, C. L., Zevin, M., Pankow, C., et al. 2016, ApJL, 832, L2
Roulet, J., & Zaldarriaga, M. 2019, MNRAS, 484, 4216
Schrøder, S. L., Batta, A., & Ramirez-Ruiz, E. 2018, ApJL, 862, L3
Spruit, H. C. 1999, A&A, 349, 189
Spruit, H. C. 2002, A&A, 381, 923
Stevenson, S., Berry, C. P. L., & Mandel, I. 2017, MNRAS, 471, 2801
Talbot, C., & Thrane, E. 2017, PhRvD, 96, 023012
The LIGO Scientific Collaboration, the Virgo Collaboration, Abbott, B. P., et al. 2018a, arXiv:1811.12907
The LIGO Scientific Collaboration, the Virgo Collaboration, Abbott, B. P., et al. 2018b, arXiv:1811.12940
Venumadhav, T., Zackay, B., Roulet, J., et al. 2019, arXiv:1904.07214
Wheeler, J. C., Kagan, D., & Chatzopoulos, E. 2015, ApJ, 799, 85
Woosley, S. E., & Heger, A. 2006, ApJ, 637, 914
Yoon, S.-C., Langer, N., & Norman, C. 2006, A&A, 460, 199
Zackay, B., Venumadhav, T., Dai, L., et al. 2019, PhRvD, 100, 023007
Zaldarriaga, M., Kushnir, D., & Kollmeier, J. A. 2018, MNRAS, 473, 4174